Inorganic Chemistry

Article

pubs.acs.org/IC

Reverse Catalase Reaction: Dioxygen Activation via Two-Electron Transfer from Hydroxide to Dioxygen Mediated By a Manganese(III) Salen Complex

Takuya Kurahashi*

Institute for Molecular Science, National Institutes of Natural Sciences, Myodaiji, Okazaki, Aichi 444-8787, Japan

Supporting Information

ABSTRACT: Although atmospheric dioxygen is regarded as the most ideal oxidant, O_2 activation for use in oxygenation reactions intrinsically requires a costly sacrificial reductant. The present study investigated the use of aqueous alkaline solution for O_2 activation. A manganese(III) salen complex, Mn^{III}(salen)(Cl), in toluene reacts with aqueous KOH solution under aerobic conditions, which yields a di-μ-oxo dimanganese(IV) salen complex, $[Mn^{IV}(salen)]_2(\mu\text{-}O)_2$. The ^{18}O isotope experiments show that $^{18}O_2$ is indeed activated to give $[Mn^{IV}(salen)]_2(\mu\text{-}^{18}O)_2$ via a peroxide intermediate. Interestingly, the $^{18}OH^-$ ion in $H_2{}^{18}O$ was also incorporated to yield $[Mn^{IV}(salen)]_2(\mu\text{-}^{18}O)_2$, which implies that a peroxide species is also generated from $^{18}OH^-$. The addition of benzyl alcohol as a stoichiometric reductant selectively inhibits the ^{18}O incorporation from $^{18}OH^-$, indicating that the reaction of Mn^{III}(salen)(Cl) with OH^- supplies the electrons for O_2 reduction. The conversion of both O_2 and OH^- to a peroxide species is exactly the reverse of a catalase-like reaction, which has a great potential as the most efficient O_2 activation. Mechanistic investigations revealed that the reaction of Mn^{III}(salen)(Cl) with OH^- generates a transient species with strong reducing ability, which effects the reduction of O_2 by means of a manganese(II) intermediate.

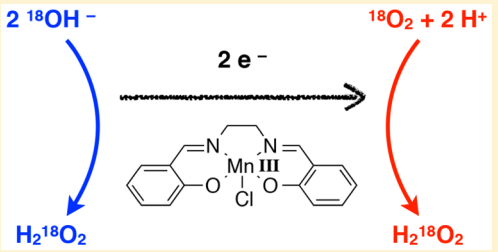

INTRODUCTION

Atmospheric dioxygen serves as the primary oxidant in numerous biological transformations.[1] Most of these transformations are promoted by transition-metal ions. Dioxygen, which is abundant and inexpensive, is undoubtedly the most ideal oxidant. But the use of dioxygen in synthetic processes for efficient substrate oxygenations remains an elusive goal. It has been an important topic to explore feasible routes of O_2 activation.

Figure 1 shows the consensus mechanism of O_2 activation, exemplified by cytochrome P-450 bearing an iron atom as the active center.[1] The first step is one-electron reduction of iron(III) that is otherwise inert for O_2. The resulting iron(II) species readily reacts with O_2 to yield an iron(III)−superoxo species. Additional one-electron reduction generates an iron(III)−hydroperoxo species, which is converted to a formally iron(V)−oxo species, an active oxidant for selective substrate oxygenations.

A variety of synthetic metal complexes have been employed to investigate the course of O_2 activation. It has been shown that some low-valent metal complexes readily react with O_2 without the need for reductants, generating distinct metal complexes bearing O_2-derived ligands.[2−5] But most of metal complexes need to be activated prior to the reaction with O_2.

A straightforward method in line with the proposed pathway in Figure 1 is the addition of reductants to supply reducing equivalents. Cytochrome P-450 enzymes utilize NADH or NADPH as a reductant for O_2 activation. In the case of synthetic iron complexes, an NADH analogue, 1-benzyl-1,4-dihydronicotinamide, was used as an electron donor for O_2 activation to generate iron(III)-hydroperoxo and iron(IV)-oxo species from iron(II) complexes.[6] It was also reported that a tetraphenylborate anion and cyclic olefins serve as an electron donor to convert iron(II) complexes to oxoiron(IV) species by activating O_2.[7−10] Other electron source materials such as

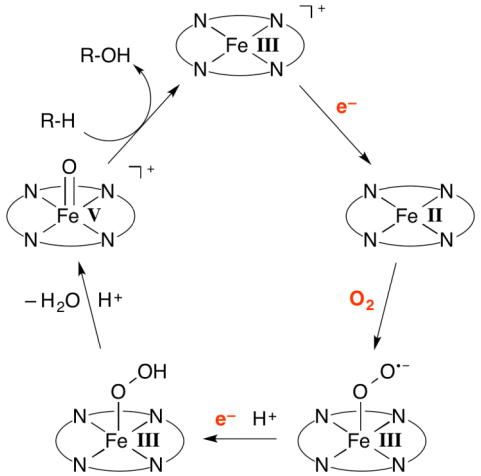

Figure 1. Dioxygen activation by an iron(III) complex, exemplified by cytochrome P450.

Received: May 7, 2015
Published: August 19, 2015

DOI: 10.1021/acs.inorgchem.5b01025
Inorg. Chem. 2015, 54, 8356−8366

ferrocene and cobaltocene are also known.[11,12] For the quantitative analysis of O_2 activation, electrochemical methods were employed.[13−15] Although the addition of reductants was successfully applied to investigate the course of biomimetic O_2 activation, it is difficult to employ this method in catalytic oxygenation reactions because of the cost of these reductants as compared with usual oxidants like hydrogen peroxide.

The use of sacrificial reductants could be circumvented changing surrounding ligands, which enables inert metal centers to react with O_2. It was reported that even changing the solvent is effective for a stable iron(II) complex to gain the reactivity for O_2.[16] A manganese(III) complex with a tetradentate bis-amido bis-alkoxo ligand undergoes air oxidation, yielding an oxomanganese(V) complex.[17] By using a corrolate trianion as a ligand, a chromium(III) complex directly reacts with O_2 to give an oxochromium(V) complex,[18] while a chromium(III) porphyrin complex can also react with O_2 upon the treatment with amines.[19] The presence of a chromium−carbon bond also increases the reactivity of chromium(III) for O_2.[20] Even the iron(III) complex becomes reactive toward O_2 with the tetraamido macrocyclic ligand.[21] It was also reported that redox-active ligands promote air oxidation of an oxorhenium-(V) complex to a dioxorhenium(VII) product.[22] In the case of photoactive iron(III) or manganese(III) complexes such as porphyrin complexes, the photoirradiation was employed for O_2 activation.[23−28]

The present study describes another attractive route of O_2 activation, in which aqueous alkaline solution is employed for O_2 activation. It has been reported that the reaction of some metal complexes with OH^- results in the one-electron reduction of metal ion.[29−33] The one-electron reduction of *p*-benzoquinones in the presence of OH^- was investigated in more detail, which clarified that the OH^- adduct anion of *p*-benzoquinone is a real electron donor and that OH^- works as a strong base or nucleophile to react with *p*-benzoquinone.[34,35] But such a reactivity of OH^- has not been applied for O_2 activation catalyzed by a metal complex. A great advantage for using OH^- in O_2 activation is that the electron release from OH^- is expected to generate H_2O_2, which is exactly the same product from the reduction of O_2. In contrast to unwanted byproducts from usual electron source materials, H_2O_2 from OH^- could be utilized as an oxidant. The formation of H_2O_2 from O_2 and OH^- is considered as the reverse of a catalase-like reaction. The reverse catalase reaction with perfect atom economy is the most efficient route of O_2 activation.

Here, a Mn^{III}(salen)(Cl) complex (manganese(III) salen complex bearing Cl as a fifth ligand), a well-known oxidation catalyst,[36] was reacted with aqueous alkaline solution in the presence of O_2. This reaction yields a di-μ-oxo dimanganese-(IV) salen complex, $[Mn^{IV}(salen)]_2(\mu\text{-}O)_2$, which is formally a product from the reaction of Mn^{III}(salen)(Cl) and H_2O_2.[37] The present study has shown that the formation of $[Mn^{IV}(salen)]_2(\mu\text{-}O)_2$ is exactly a consequence of the reverse catalase reaction. Mechanistic details clarified in the present study are of fundamental importance for further studies to explore aerobic oxygenation reactions using the reverse catalase reaction as a key O_2 activation step.

RESULTS

Characterization of ^{18}O-Labeled $[Mn^{IV}(salen)]_2(\mu\text{-}O)_2$. As previously reported,[38] the $[Mn^{IV}(salen)]_2(\mu\text{-}O)_2$ complex is prepared by the reaction of Mn^{III}(salen)(Cl) in toluene with 2.0 M KOH aqueous solution. The $[Mn^{IV}(salen)]_2(\mu\text{-}O)_2$ complex was fully characterized with various techniques including X-ray crystallography. Here, the same reaction was conducted under the $^{18}O_2$ atmosphere using 2.0 M $Na^{18}OH$ in $H_2{}^{18}O$ (Scheme 1).

Scheme 1. Reaction of Mn^{III}(salen) (Cl) with ^{18}O-Labeled Aqueous Alkaline Solution under $^{18}O_2$ Atmosphere

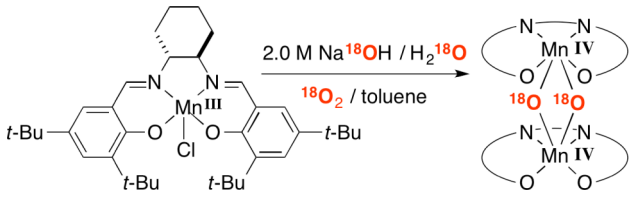

Mass spectrometry shows that the signal at m/z 1231.72 for $[Mn^{IV}(salen)]_2(\mu\text{-}O)_2$ cleanly shifts to m/z 1235.73, indicating that two ^{18}O atoms are incorporated (Figure 2). Resonance

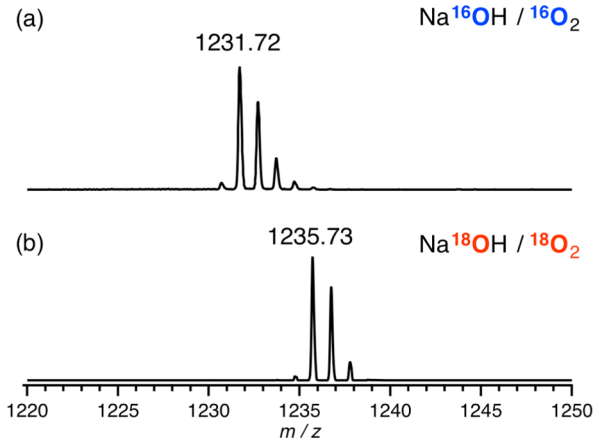

Figure 2. ESI mass spectra of $[Mn^{IV}(salen)]_2(\mu\text{-}O)_2$ complexes that are prepared under the following conditions: (a) 2.0 M $Na^{16}OH$ in $H_2{}^{16}O$ under $^{16}O_2$ atmosphere and (b) 2.0 M $Na^{18}OH$ in $H_2{}^{18}O$ under $^{18}O_2$ atmosphere.

Raman (rR) spectra of $[Mn^{IV}(salen)]_2(\mu\text{-}O)_2$ were measured with excitation at 532 nm (Figure 3), which is a lowest-energy tail of the visible absorption of $[Mn^{IV}(salen)]_2(\mu\text{-}O)_2$. The intense band at 636 cm^{-1} for $[Mn^{IV}(salen)]_2(\mu\text{-}O)_2$ shifts to 611 cm^{-1} when $Na^{18}OH$ and $^{18}O_2$ are used. The isotope-sensitive feature in the 600−700 cm^{-1} region has proven to be diagnostic of double ^{18}O substitution in the di-μ-oxo dimetal core of Cu,[39] Fe,[40] and Mn.[41] Thus, the ^{18}O atoms from $Na^{18}OH$ and $^{18}O_2$ are incorporated to the two bridging oxo ligands in $[Mn^{IV}(salen)]_2(\mu\text{-}O)_2$. Additionally, double ^{18}O substitution shifts the band at 1284 cm^{-1} to 1230 cm^{-1}. Isotope-sensitive bands in such a high-frequency region have not been reported for other di-μ-oxo dimetal complexes. This vibrational mode is most probably assigned as the first overtone of the 636 cm^{-1} mode.

The isotope-sensitive region around 600 cm^{-1} was investigated in more detail by rR and IR (infrared) spectra (Figure 4). In addition to the intense rR band at 636 cm^{-1}, a weak rR band at 580 cm^{-1} shifts to 567 cm^{-1} upon double ^{18}O isotope substitution. The isotope shift for the rR band at 580 cm^{-1} (13 cm^{-1}) is significantly smaller than that for the rR band at 636 cm^{-1} (25 cm^{-1}). IR spectra also show two isotope-sensitive bands at 643 and 584 cm^{-1}, which shift to 618 and

DOI: 10.1021/acs.inorgchem.5b01025
Inorg. Chem. 2015, 54, 8356−8366

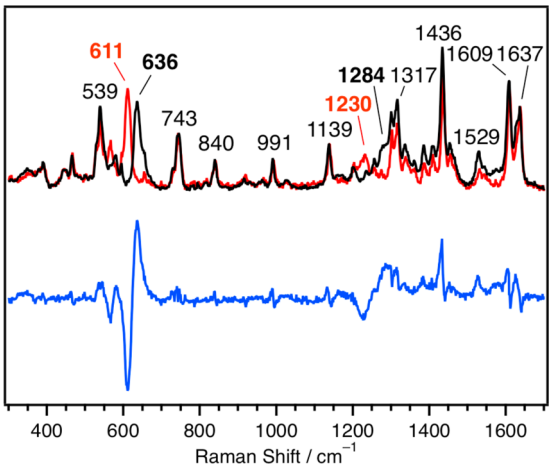

Figure 3. Resonance Raman spectra of solid samples of $[Mn^{IV}(salen)]_2(\mu\text{-}O)_2$ complexes that are prepared under $^{16}O_2$ atmosphere using 2.0 M $Na^{16}OH$ in $H_2{}^{16}O$ (black) and under $^{18}O_2$ atmosphere using 2.0 M $Na^{18}OH$ in $H_2{}^{18}O$ (red). The blue line shows the difference ($^{16}O - {}^{18}O$) spectrum. The spectra were obtained at room temperature with excitation at 532 nm.

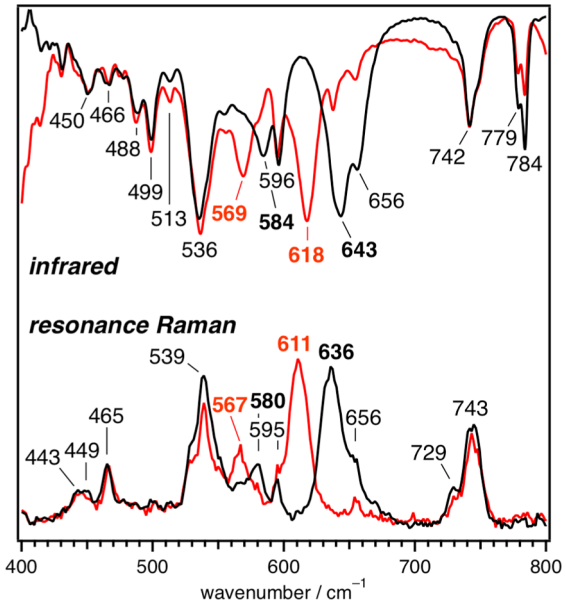

Figure 4. Resonance Raman and IR spectra of $[Mn^{IV}(salen)]_2(\mu\text{-}O)_2$ complexes that are prepared under $^{16}O_2$ atmosphere using 2.0 M $Na^{16}OH$ in $H_2{}^{16}O$ (black) and under $^{18}O_2$ atmosphere using 2.0 M $Na^{18}OH$ in $H_2{}^{18}O$ (red). The resonance Raman spectra were obtained for solid samples at room temperature with excitation at 532 nm. The IR spectra were obtained for KBr pellets at a resolution of 2 cm^{-1} as a sum of 32 scans.

569 cm^{-1}, respectively. The isotope shifts of these two IR bands are 25 and 15 cm^{-1}, respectively.

As already reported in the previous rR studies on the di-μ-oxo dimetal core,[39,40] the rR band at 636 cm^{-1} for $[Mn^{IV}(salen)]_2(\mu\text{-}O)_2$ is readily assigned as a symmetric A_g vibration of the di-μ-oxo dimanganese(IV) core, in which all Mn−O bonds stretch in phase. The observed isotope shift is in excellent agreement with the predicted value from density functional theory calculations reported for the $[Mn^{IV}(NH_3)_4]_2(\mu\text{-}O)_2$ model (theoretical, 26 cm^{-1} shift at 629 cm^{-1}; experimental, 25 cm^{-1} shift at 636 cm^{-1}).[42] The isotope-sensitive IR band at 643 cm^{-1}, however, is assigned as an asymmetric B_{3u} vibration (theoretical, 23 cm^{-1} shift at 615 cm^{-1}; experimental, 25 cm^{-1} shift at 643 cm^{-1}). The vibrational analysis of the $[Mn^{IV}(NH_3)_4]_2(\mu\text{-}O)_2$ model also indicates that the IR band at 584 cm^{-1} is assigned as an asymmetric B_{2u} vibration, because the theoretical and experimental isotope shifts are in reasonably good agreement (theoretical, 11 cm^{-1} shift at 580 cm^{-1}; experimental, 15 cm^{-1} shift at 584 cm^{-1}). Among the possible Raman-allowed vibrations predicted from normal coordinate analyses, the rR band at 580 cm^{-1} is best assigned as arising from the symmetric B_{1g} vibration. But the predicted values are substantially different (theoretical, 17 cm^{-1} shift at 478 cm^{-1}; experimental, 13 cm^{-1} shift at 580 cm^{-1}). This is probably because the salen ligand with lower symmetry than the NH_3 model may participate in the coupling with this vibrational mode, as reported in the in-depth analysis for rR spectra of di-μ-oxo dicopper cores.[39]

^{18}O-Labeling Experiments. To investigate the ^{18}O incorporation from $^{18}O_2$ gas, the $[Mn^{IV}(salen)]_2(\mu\text{-}O)_2$ complex was prepared under the $^{18}O_2$ atmosphere using nonlabeled NaOH in H_2O. The mass spectrum shows that two signals are observed at m/z 1231.73 and 1235.75 (Figure 5a). The rR measurement also shows two bands at 636 and 611 cm^{-1} (Figure 5a), indicating that the resulting sample is a mixture of $[Mn^{IV}(salen)]_2(\mu\text{-}{}^{16}O)_2$ and $[Mn^{IV}(salen)]_2$-

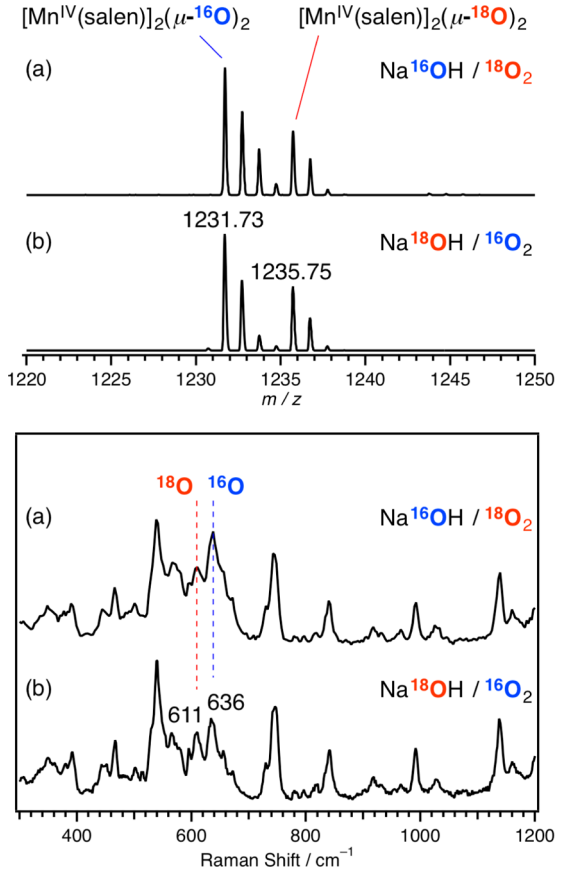

Figure 5. Mass and resonance Raman spectra of $[Mn^{IV}(salen)]_2(\mu\text{-}O)_2$ complexes that are prepared (a) under the $^{18}O_2$ atmosphere using the nonlabeled 2.0 M NaOH in H_2O and (b) under the nonlabeled O_2 atmosphere using 2.0 M $Na^{18}OH$ in $H_2{}^{18}O$. The resonance Raman spectra were obtained for solid samples at room temperature with excitation at 532 nm.

DOI: 10.1021/acs.inorgchem.5b01025
Inorg. Chem. 2015, 54, 8356−8366

(μ-^{18}O)$_2$. Thus, the $^{18}O_2$ molecule is activated during the dimerization of Mn^{III}(salen)(Cl) and is incorporated into the product. The ratio of [Mn^{IV}(salen)]$_2$(μ-^{16}O)$_2$ and [Mn^{IV}(salen)]$_2$(μ-^{18}O)$_2$ is 7:3 as estimated from the rR spectrum. It was confirmed that the bridging ^{18}O atoms in [Mn^{IV}(salen)]$_2$(μ-^{18}O)$_2$ are not exchangeable with O_2 and H_2O during handling the sample. Then, the formation of [Mn^{IV}(salen)]$_2$(μ-^{16}O)$_2$ indicates that O_2 molecule is not a sole source of the bridging oxygen atom.

Subsequently, the dimerization of Mn^{III}(salen)(Cl) was conducted under the nonlabeled O_2 atmosphere using Na^{18}OH in $H_2{}^{18}O$. Quite interestingly, the mass and rR spectra show that the resulting sample is a mixture of [Mn^{IV}(salen)]$_2$(μ-^{16}O)$_2$ and [Mn^{IV}(salen)]$_2$(μ-^{18}O)$_2$ (Figure 5b), indicating that the ^{18}O atom is also incorporated from $^{18}OH^-$. The partially labeled [Mn^{IV}(salen)]$_2$(μ-^{16}O)(μ-^{18}O) is not formed at all. The rR spectrum shows that the ratio of [Mn^{IV}(salen)]$_2$(μ-^{16}O)$_2$ and [Mn^{IV}(salen)]$_2$(μ-^{18}O)$_2$ is 6:4.

Table 1 summarizes ^{18}O incorporation in the dimerization reaction of Mn^{III}(salen)(Cl) to [Mn^{IV}(salen)]$_2$(μ-O)$_2$. Accord-

Table 1. ^{18}O Incorporation for the Reaction of Mn^{III}(salen)(Cl) in Toluene with Aqueous Alkaline Solution

	Na^{16}OH	Na^{18}OH
$^{16}O_2$	[Mn^{IV}(salen)]$_2$(μ-^{16}O)$_2$	[Mn^{IV}(salen)]$_2$(μ-^{16}O)$_2$ (60%) [Mn^{IV}(salen)]$_2$(μ-^{18}O)$_2$ (40%)
$^{18}O_2$	[Mn^{IV}(salen)]$_2$(μ-^{16}O)$_2$ (70%) [Mn^{IV}(salen)]$_2$(μ-^{18}O)$_2$ (30%)	[Mn^{IV}(salen)]$_2$(μ-^{18}O)$_2$

ing to Table 1, 40% of the bridging oxygen in [Mn^{IV}(salen)]$_2$(μ-O)$_2$ comes from OH^- in H_2O. Then, the origin of the remaining 60% should be O_2 gas. But the isotope experiment shows that only 30% of the bridging oxygen is ^{18}O-labeled under $^{18}O_2$ atmosphere. Low ^{18}O incorporation is probably due to low concentration of $^{18}O_2$ in the solvent, because the solvent could not be exposed to $^{18}O_2$ atmosphere for a long time to avoid the contamination of $^{16}O_2$.

Electron Source for O_2 Activation. The ^{18}O experiments provide clear evidence that O_2 molecule is activated. The next important point is the source of two electrons that are utilized for O_2 activation. To clarify the electron source, the aerobic oxidation of Mn^{III}(salen)(Cl) was conducted in the presence of an added reductant, which was intended to block the original electron-releasing reaction.

The toluene solution of Mn^{III}(salen)(Cl) was reacted with 2.0 M KOH aqueous solution in the presence of 1 equiv of triphenylphosphine, methyl phenyl sulfide, or cyclohexene. Gas chromatography−mass spectrometry (GC-MS) analyses showed no oxidized product (triphenylphosphine oxide, methyl phenyl sulfoxide, cyclohexene oxide, 2-cyclohexene-1-ol, 2-cyclohexene-1-one), and the yields of [Mn^{IV}(salen)]$_2$(μ-O)$_2$ are almost the same as compared to the original reaction in the absence of these substrates. In contrast, the aerobic oxidation of Mn^{III}(salen)(Cl) in the presence of 1 equiv of benzyl alcohol generates benzaldehyde in 43 ± 7% yield as shown by ^{1}H NMR (Figure S1, Supporting Information). The oxidation of benzyl alcohol to benzaldehyde indicates that benzyl alcohol functions as a two-electron donor in this system. The yield of [Mn^{IV}(salen)]$_2$(μ-O)$_2$ slightly decreases from 59 ± 10% without benzyl alcohol to 43 ± 7% in the presence of benzyl alcohol.

The ^{18}O incorporation was then investigated using Na^{18}OH in $H_2{}^{18}O$ under nonlabeled O_2 atmosphere in the presence of 1 equiv of benzyl alcohol. In the absence of benzyl alcohol, 40% of [Mn^{IV}(salen)]$_2$(μ-O)$_2$ is ^{18}O-labeled (Table 1), but in the presence of benzyl alcohol, none of [Mn^{IV}(salen)]$_2$(μ-O)$_2$ is ^{18}O-labeled as shown by mass and rR spectra (Figure S2). This result is a clear indication that the two-electron oxidation of benzyl alcohol competes with the reaction of Mn^{III}(salen)(Cl) with $^{18}OH^-$ to produce [Mn^{IV}(salen)]$_2$(μ-^{18}O)$_2$. Therefore, in the original reaction without benzyl alcohol, the two electrons required for O_2 activation are provided from the reaction of Mn^{III}(salen)(Cl) and OH^-.

Reaction with Weak Base. A Mn^{III}(salen) complex was reacted with weak base instead of strong base such as KOH and NaOH to investigate whether O_2 activation may occur or not. The Mn^{III}(salen)(Cl) complex was reacted with basic alumina containing water (20 wt %), which is much weaker base than KOH and NaOH. But the Mn^{III}(salen)(Cl) complex remains intact for 24 h at room temperature. Then, the Mn^{III}(salen)(OTf) complex having a weakly coordinating trifluoromethanesulfonate (OTf) as an axial ligand was employed for the reaction with basic alumina containing water, which generates a distinct species. For the characterization of the product, the selectively deuterated Mn^{III}(salen-d_4)(OTf) and Mn^{III}(salen-d_2)(OTf) complexes (Chart S1) were utilized for ^{2}H NMR measurements. In salen-d_4, ^{2}H atoms are selectively incorporated into the phenolate rings (80% D) and the *tert*-butyl groups (7% D). The salen-d_2 ligand is selectively deuterated at the 7/7′ positions (99.5% D).

^{1}H and ^{2}H NMR spectra (Figure 6a,b) show that the phenolate protons in the product appear at 7.0/8.0 and −9.0/−9.6 ppm. The ^{2}H NMR signals from the azomethine are observed at −169/−252 ppm (Figure 6c). The signals from the left and right phenolates and azomethines are observed separately, indicating that the left and right halves of the salen complex are located in a different environment. Paramagnetic shifts of the product are much smaller than those of the starting Mn^{III}(salen)(OTf) complex (phenolate protons, 7.4, −31.1 ppm; azomethine proton, −445 ppm[43]). The ^{1}H and ^{2}H NMR signals of the product are different from those of [Mn^{IV}(salen)]$_2$(μ-O)$_2$ (phenolate protons, 8.8, 8.3, 6.4, 4.3 ppm; azomethine protons, −18.9, −37.6 ppm[38]), indicating that the [Mn^{IV}(salen)]$_2$(μ-O)$_2$ complex is not formed in the reaction of Mn^{III}(salen)(OTf) with basic alumina containing water. The absorption spectrum of the product is also different from that of [Mn^{IV}(salen)]$_2$(μ-O)$_2$ (Figure S3).

The CH_2Cl_2 solution of the product complex was washed with D_2O and was then analyzed with ^{2}H NMR (Figure 6d). Importantly, a broad ^{2}H NMR signal is observed at 312 ppm. The observation of a D_2O-exchangable signal at largely shifted position is a clear indication that the product complex has a labile proton in close proximity to the manganese center. Temperature dependence of all the ^{2}H NMR signals yields similar curved Curie plot (Figure S4).

The starting Mn^{III}(salen)(OTf) complex shows perpendicular- and parallel-mode electron paramagnetic resonance (EPR) signal at g = 8.0, which disappears after the reaction with basic alumina containing water (Figure S5). Neither perpendicular- nor parallel-mode EPR signal is observed for the product, indicating that the product is a manganese dimer of the same oxidation state. Mass spectrometry shows an ion signal at m/z 1215.48, which corresponds to [[Mn^{III}(salen)]$_2$(OH)]$^+$ (Figure S6). Elemental analysis shows a composition of [Mn^{III}(salen)]$_2$-

DOI: 10.1021/acs.inorgchem.5b01025
Inorg. Chem. 2015, 54, 8356−8366

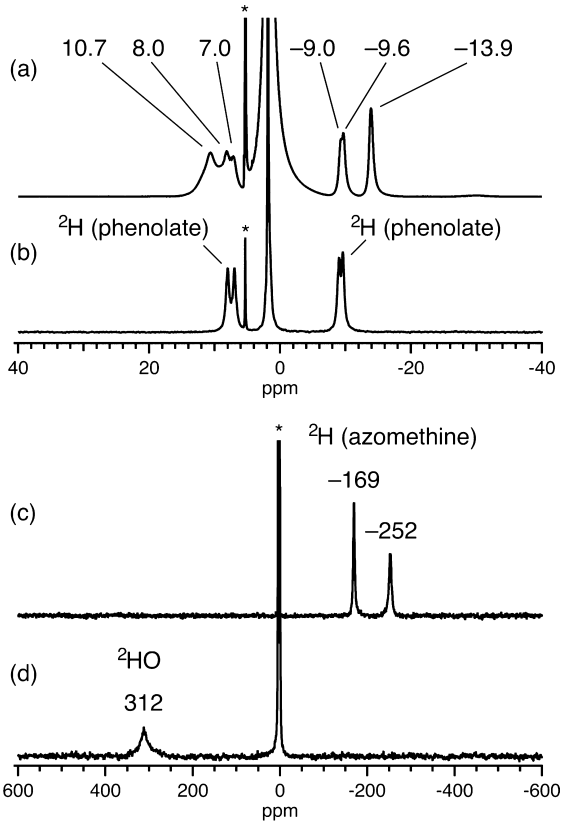

Figure 6. (a) ^{1}H NMR spectrum of $[Mn^{III}(salen)]_2(\mu$-OH)(OTf) in CD_2Cl_2. (b) ^{2}H NMR spectrum of $[Mn^{III}(salen\text{-}d_4)]_2(\mu$-OH)(OTf) in CH_2Cl_2. (c) ^{2}H NMR spectrum of $[Mn^{III}(salen\text{-}d_2)]_2(\mu$-OH)(OTf) in CH_2Cl_2. (d) ^{2}H NMR spectrum of $[Mn^{III}(salen)]_2(\mu$-OD)(OTf) in CH_2Cl_2. Measurements were performed at 298 K for the 20 mM solution. In salen-d_4, ^{2}H atoms are selectively incorporated into the phenolate rings (80% D) and the *tert*-butyl groups (7% D). The salen-d_2 ligand is selectively deuterated at the 7/7′ positions (99.5% D). The signals denoted with an asterisk come from residual $CHDCl_2$ and are referenced to 5.32 ppm.

(OH)(OTf). According to these data, the product is a μ-OH bridged Mn^{III} dimer, $[Mn^{III}(salen)]_2(\mu$-OH)(OTf). Resonance Raman and IR measurements were performed for $[Mn^{III}(salen)]_2(\mu$-OH)(OTf), but an ^{18}O- or ^{2}H-sensitive band was not observed (Figures S7 and S8).

The conversion from Mn^{III}(salen)(OTf) to $[Mn^{III}(salen)]_2(\mu$-OH)(OTf) does not accompany the redox of manganese ion. Higher concentration of OH^- such as NaOH and KOH aqueous solution is necessary to initiate the redox reaction from Mn^{III}(salen)(Cl) to $[Mn^{IV}(salen)]_2(\mu\text{-}O)_2$. Interestingly, the reaction of $[Mn^{III}(salen)]_2(\mu$-OH)(OTf) with 2.0 M KOH aqueous solution does not produce the $[Mn^{IV}(salen)]_2(\mu\text{-}O)_2$ complex, indicating that a monomeric manganese center in the starting complex is crucial for the present reaction.

Effect of Added Oxidants. To investigate a key redox reaction, the reaction of Mn^{III}(salen)(Cl) with 2.0 M KOH aqueous solution was conducted in the presence of quinones with different redox potentials. Addition of 1 equiv of *p*-benzoquinone (E_c, cathodic reduction peak potential, −1.042 V vs ferrocene/ferrocenium couple, Fc/Fc^+) does not alter the reaction, and the $[Mn^{IV}(salen)]_2(\mu\text{-}O)_2$ product is obtained in 63 ± 9% yield, as compared with 59 ± 10% yield in the absence of *p*-benzoquinone (Table 2). Addition of 1 equiv of 2,5-dichloro-1,4-benzoquinone with higher oxidizing power (E_c, −0.711 V vs Fc/Fc^+) causes decreased yield of $[Mn^{IV}(salen)]_2(\mu\text{-}O)_2$ (33 ± 3%). Quite interestingly, in the presence of 1 equiv of chloranil (E_c, −0.494 V vs Fc/Fc^+), the $[Mn^{IV}(salen)]_2(\mu\text{-}O)_2$ complex is not formed at all. Instead, the major product shows a ^{1}H NMR spectrum that is almost identical with that of $[Mn^{III}(salen)]_2(\mu$-OH)(OTf) prepared from the reaction with alumina containing water (20 wt %) (Figure S10). This indicates that the product is $[Mn^{III}(salen)]_2(\mu$-OH)(X), where X is a counterion but is not determined. Only 1 equiv of chloranil completely changes the reaction from the redox process generating $[Mn^{IV}(salen)]_2(\mu\text{-}O)_2$ to the nonredox process generating $[Mn^{III}(salen)]_2(\mu$-OH)(X). A dramatic effect of an oxidant (chloranil) as compared with a reductant (benzyl alcohol) indicates that a transient species with reducing ability plays a key role in the formation of $[Mn^{IV}(salen)]_2(\mu\text{-}O)_2$.

Table 2. Effect of Quinones on the Formation of $[Mn^{IV}(salen)]_2(\mu\text{-}O)_2$[a]

quinone	redox potential[b] (V vs Fc/Fc^+)	yield of $[Mn^{IV}(salen)]_2(\mu\text{-}O)_2$[c] (%)
no additive		59 ± 10
p-benzoquinone	−0.966 (−1.042/−0.889)	63 ± 9
2,5-dichloro-1,4-benzoquinone	−0.644 (−0.711/−0.576)	33 ± 3
chloranil	−0.437 (−0.494/−0.380)	0[d]

[a] Mn^{III}(salen)(Cl) (50 mg) and 1 equiv of quinone in toluene (5 mL) was washed with 2.0 M aqueous KOH solution (5 mL). [b] Redox potentials of quinones were determined with cyclic voltammetry in CH_2Cl_2 containing 0.1 M Bu_4NOTf (Figure S9). Redox potentials are shown as $E_{1/2}$ values as well as E_c and E_a values in parentheses, where E_c is a cathodic reduction peak potential, E_a is an anodic oxidation peak potential, and $E_{1/2}$ is an averaged value of E_c and E_a. [c] Averaged values from three independent experiments. [d] the $[Mn^{III}(salen)]_2(\mu$-OH)(X) complex is formed as a major product (Figure S10).

Anaerobic Reaction. To investigate the key reducing intermediate that is responsible for the two-electron reduction of O_2, the reaction of Mn^{III}(salen)(Cl) with OH^- was performed in the absence of O_2. Then, the toluene solution of Mn^{III}(salen)(Cl) was washed with 2.0 M KOH aqueous solution under Ar atmosphere. After the toluene solution was dried, insoluble materials in toluene were carefully removed using a membrane filter, and the resulting solution was analyzed with EPR, ^{1}H NMR spectroscopy, and mass spectrometry.

Figure 7 shows the perpendicular-mode X-band EPR spectrum. An intense 16-line signal at g = 2 is observed under anaerobic conditions. This signal is persistent under Ar atmosphere for hours at room temperature but immediately disappears in contact with air. Variable-temperature EPR measurements from 4 to 15 K show that the intensity of the 16-line signal simply decreases and that no other signal is observed (Figure S11). The single signal at g = 2 indicates that the species that is generated under Ar has the S = 1/2 ground state. The 16-line hyperfine structure is a clear indication that the system contains two inequivalent ^{55}Mn (I = 5/2) nuclei. Thus, the species that is formed from Mn^{III}(salen)(Cl) and OH^- under anaerobic conditions is a localized mixed-valence Mn^{II}/Mn^{III} or Mn^{III}/Mn^{IV} dimer in which two Mn ions are involved in strong antiferromagnetic electron exchange coupling.

To distinguish Mn^{II}/Mn^{III} and Mn^{III}/Mn^{IV} complexes, the 16-line EPR signal was analyzed to obtain hyperfine parameters.

DOI: 10.1021/acs.inorgchem.5b01025
Inorg. Chem. 2015, 54, 8356−8366

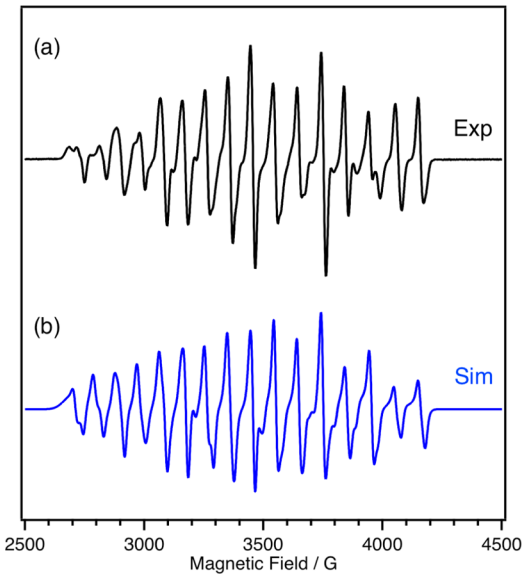

Figure 7. (a) X-band EPR spectrum of $[Mn^{II}(salen)][Mn^{III}(salen)](\mu$-OH) in toluene (20 mM), generated by washing the toluene solution of $Mn^{III}(salen)$ (Cl) with aqueous 2.0 M KOH solution under Ar atmosphere. Conditions: temperature, 4 K; microwave frequency, 9.688 GHz; microwave power, 0.10 mW; modulation amplitude, 1.0 G; time constant, 163.84 ms; conversion time, 74.93 ms. (b) Simulation curve with g values and Mn hyperfine parameters listed in Table 3.

It was demonstrated that a Mn^{II}/Mn^{III} pair exhibits a 25% larger ^{55}Mn hyperfine field than a Mn^{III}/Mn^{IV} pair in the case of a manganese porphyrin.[44] The simulation was done by using the EasySpin software,[45] which solves the following spin Hamiltonian:

$$H = bB\cdot g\cdot S + S\cdot A_1\cdot I_1 - g_n b_n B\cdot I_1 + S\cdot A_2\cdot I_2 - g_n b_n B\cdot I_2$$

where S is the total electron spin, B is the external magnetic field, A is the intrinsic hyperfine tensor, I is the nuclear spin, g is the g factor, and β is the Bohr magneton, g_n is the nuclear g factor, and β_n is the nuclear magneton. The subscripts 1 and 2 refer to the two inequivalent manganese ions.

As shown in Figure 7, a satisfactory good fit was obtained using the parameters summarized in Table 3. Table 3 also lists the hyperfine parameters of previous Mn^{II}/Mn^{III} and Mn^{III}/Mn^{IV} complexes having the S = 1/2 ground state. The hyperfine parameters obtained from the present simulation are close to the parameters of Mn^{II}/Mn^{III} complexes[46−48] rather than the parameters of Mn^{III}/Mn^{IV} complexes.[49] It is thus indicated that this species is assigned as the Mn^{II}/Mn^{III} complex. The mass spectrum of this species shows a predominant signal at m/z 1215.75, which corresponds to the $[[Mn^{III}(salen)]_2(OH)]^+$ ion (Figure S12). Therefore, the species that is generated from $Mn^{III}(salen)(Cl)$ and OH^- under anaerobic conditions is a μ-OH-bridged Mn^{II}/Mn^{III} dimer, $[Mn^{II}(salen)][Mn^{III}(salen)](\mu$-OH). The yield of $[Mn^{II}(salen)][Mn^{III}(salen)](\mu$-OH) is ca. 30%; namely, only 15% of $Mn^{III}(salen)(Cl)$ is reduced to $Mn^{II}(salen)$, as estimated by double integration of EPR signals using the Mn^{III}/Mn^{IV} complex $[OH_2(terpy)Mn(\mu\text{-}O)_2Mn(tertpy)OH_2]$ (terpy = 2,2′:6′,2″-terpyridine)[50] as a standard. A low yield is due to the demetalation of the Mn(salen) complex under anaerobic conditions as indicated by the formation of the free salen ligand (Figure S13), although under aerobic conditions, the demetalation is not a serious problem (Figure S14).

The anaerobic reaction was then investigated with ^{1}H NMR (Figure S13). Although the redox reaction generating $[Mn^{II}(salen)][Mn^{III}(salen)](\mu$-OH) occurs, the $[Mn^{IV}(salen)]_2(\mu\text{-}O)_2$ complex is not formed at all under anaerobic conditions. But upon exposure to air, ^{1}H NMR signals of $[Mn^{IV}(salen)]_2(\mu\text{-}O)_2$ appear within a minute, which is synchronized with the disappearance of the 16-line EPR signal. This indicates that the $[Mn^{II}(salen)][Mn^{III}(salen)](\mu$-OH) complex readily reacts with O_2 to yield $[Mn^{IV}(salen)]_2(\mu\text{-}O)_2$. The formation of the di-μ-oxo dimanganese(IV) dimer of salen and related ligands from the reaction of manganese(II) species with O_2 was previously well-documented.[51−54]

Under aerobic conditions, the reaction using $^{18}OH^-$ yields $[Mn^{IV}(salen)]_2(\mu\text{-}^{18}O)_2$. The ^{18}O incorporation under anaerobic conditions was then investigated. When $^{18}OH^-$ is utilized in the reaction of $Mn^{III}(salen)(Cl)$ under Ar, no ^{18}O incorporation was observed in the $[Mn^{IV}(salen)]_2(\mu\text{-}O)_2$ product after the workup under air (Figure S15). This result indicates that

Table 3. Electron Paramagnetic Resonance Parameters of Mn^{II}/Mn^{III} and Mn^{III}/Mn^{IV} Complexes[a]

		Mn_1	Mn_2	
complex[b]	g_x, g_y, g_z	$\lvert A_x\rvert$, $\lvert A_y\rvert$, $\lvert A_z\rvert$, 1×10^{-4} cm^{-1}	$\lvert A_x\rvert$, $\lvert A_y\rvert$, $\lvert A_z\rvert$, 1×10^{-4} cm^{-1}	reference
$[Mn^{II}(salen)][Mn^{III}(salen)](\mu$-OH)	1.998, 2.002, 2.037	88, 86, 136	175, 188, 128	this work
$[Mn^{II}Mn^{III}(L_1)(\mu\text{-}OAc)_2](ClO_4)$	1.753, 1.938, 2.015	61, 63, 123	157, 120, 262	46
$[Mn^{II}Mn^{III}(L_2)(\mu\text{-}OAc)_2](ClO_4)$	1.844, 1.932, 2.005	60, 66, 122	157, 146, 259	47
$[Mn^{II}Mn^{III}(L_3)(\mu\text{-}OAc)_2](ClO_4)_2$	1.905, 1.905, 2.022	73, 73, 106	153, 153, 245	48
$[Mn^{II}Mn^{III}(L_4)(\mu\text{-}OAc)_2](ClO_4)_2$	1.813, 1.883, 2.026	65, 65, 113	145, 145, 267	48
$[Mn^{III}/Mn^{IV}(\mu\text{-}O)_2(\mu\text{-}OAc)dtne](BPh_4)_2$	1.984, 1.997, 2.001	71, 65, 74	99, 157, 136	47
$[Mn^{III}/Mn^{IV}(\mu\text{-}O)_2(\mu\text{-}OAc)mdtn](BPh_4)_2$	1.983, 1.996, 2.003	72, 65, 74	105, 161, 140	49
$[Mn^{III}/Mn^{IV}(\mu\text{-}O)_2(\mu\text{-}OAc)tacn_2](BPh_4)_2$	1.985, 2.001, 2.003	75, 66, 74	98, 153, 137	49
$[Mn^{III}/Mn^{IV}(\mu\text{-}O)_2bipy_4](ClO_4)_3$	1.982, 1.993, 1.999	78, 72, 70	125, 160, 167	49
$[Mn^{III}/Mn^{IV}(\mu\text{-}O)_2phen_4](ClO_4)_3$	1.982, 1.994, 1.999	78, 72, 71	124, 160, 167	49

[a]The Mn_1 and Mn_2 are assigned to Mn^{III} and Mn^{II} ions in the case of Mn^{II}/Mn^{III} complexes, respectively. The Mn_1 and Mn_2 are assigned to Mn^{IV} and Mn^{III} ions in the case of Mn^{III}/Mn^{IV} complexes, respectively. [b]L_1 = dianion of 2-(((3-((bis(pyridin-2-ylmethyl)amino)methyl)-2-hydroxy-5-methylbenzyl)(pyridin-2-ylmethyl)amino)-methyl) phenol. L_2 = dianion of 2-{[*N*,*N*-bis(2-pyridylmethyl)amino]methyl}-6-{[*N*-(3,5-di-*tert*-butyl-2-hydroxybenzyl)-*N*-(2-pyridylmethyl)-amino]methyl}-4-methylphenol. L_3 = monoanion of 2,6-bis(1,4,7-triazacyclonon-1-ylmethyl)-4-methylphenol. L_4 = monoanion of 2,6-bis[bis(2-pyridylmethyl)aminomethyl]-4-methylphenol. dtne = 1,2-bis(1,4,7-triazacyclononyl)ethane. mdtn = 1,2-bis(4,7-dimethyl-1,4,7-triazacyclononyl)ethane. tacn = 1,4,7-triazacyclononane. bipy = bipyridine. phen = *o*-phenanthrolin.

DOI: 10.1021/acs.inorgchem.5b01025
Inorg. Chem. 2015, 54, 8356−8366

Scheme 2. Proposed Reaction Sequences of O_2 Activation in the Presence of OH^-

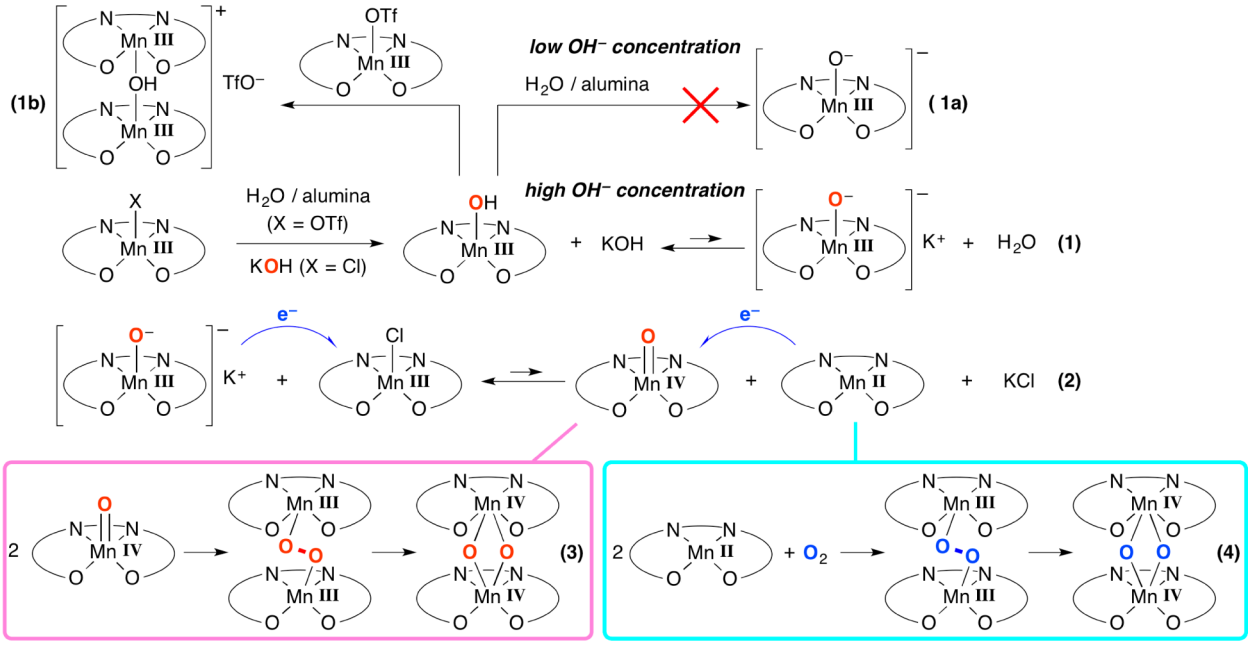

the formation of $[Mn^{IV}(salen)]_2(\mu\text{-}O)_2$ from the reaction of $Mn^{III}(salen)(Cl)$ with OH^- requires O_2 atmosphere. In other words, the two-electron oxidation of OH^- is coupled with the two-electron reduction of O_2.

DISCUSSION

Proposed Mechanism for O_2 Activation via Two-Electron Transfer from Hydroxide to Dioxygen. According to the ^{18}O-labeling experiments, the formation of $[Mn^{IV}(salen)]_2(\mu\text{-}O)_2$ is the consequence of two different pathways where the bridging oxygen atoms are derived from O_2 or OH^-. To account for the present observation, the reaction sequences shown in Scheme 2 are proposed. The first step is the reaction of $Mn^{III}(salen)(Cl)$ with 2 equiv of KOH to generate a $[Mn^{III}(salen)(O)]^-$ species as a key intermediate with strong reducing ability (eq 1), where the OH^- ion is acting as a strong base.[34,35,55] When basic alumina containing water is utilized as a base, the $Mn^{III}(salen)(Cl)$ complex is not converted to $Mn^{III}(salen)(OH)$. The $Mn^{III}(salen)(OTf)$ complex bearing a weakly coordinating OTf ligand can be converted to $Mn^{III}(salen)(OH)$, but the $[Mn^{III}(salen)(O)]^-$ species may not be generated because of low OH^- concentration (eq 1a). Instead, the dimerization reaction occurs to give $[Mn^{III}(salen)]_2(\mu\text{-}OH)(OTf)$ (eq 1b).

The critical role of a reducing species is strongly suggested by the reactions in the presence of quinones with increasing oxidizing ability, which decrease the yield of $[Mn^{IV}(salen)]_2(\mu\text{-}O)_2$ in a stepwise manner. Only 1 equiv of 2,5-dichloro-1,4-benzoquinone decreases the yield of $[Mn^{IV}(salen)]_2(\mu\text{-}O)_2$, and 1 equiv of chloranil completely prevents the formation of $[Mn^{IV}(salen)]_2(\mu\text{-}O)_2$. Although the $[Mn^{III}(salen)(O)]^-$ complex could not be synthesized and the exact redox properties are unknown, the reducing power of $[Mn^{III}(salen)(O)]^-$ is well above the cathodic reduction peak potential of 2,5-dichloro-1,4-benzoquinone (−0.711 V vs Fc/Fc^+) and chloranil (−0.494 V vs Fc/Fc^+). The only example of a monomeric manganese(III)−oxo complex was synthesized by Borovik and co-workers by use of peripheral hydrogen bonding to stabilize the oxo ligand.[56−58] According to their studies, the Mn^{III}/Mn^{IV} couple of the manganese(III)-oxo is −1.0 V, and the Mn^{IV}/Mn^{V} couple is −0.076 V vs Fc/Fc^+. In the present O_2 activation, the $[Mn^{III}(salen)(O)]^-$ complex is the best candidate for the reducing species.

The next step is the one-electron reduction of $Mn^{III}(salen)(Cl)$ by $[Mn^{III}(salen)(O)]^-$, which reversibly generates $Mn^{II}(salen)$ and $Mn^{IV}(salen)(O)$ (eq 2). The possibility to reduce O_2 to $O_2^{\bullet-}$ seems unlikely, because the cathodic reduction peak potential of $Mn^{III}(salen)(Cl)$ (−1.148 V vs Fc/Fc^+) is less negative than that of O_2 (−1.622 V vs Fc/Fc^+; Figure S16). Subsequently, the $Mn^{II}(salen)$ complex immediately reacts with O_2 to give $[Mn^{IV}(salen)]_2(\mu\text{-}O)_2$, in which the bridging oxygen atoms are derived from O_2 (eq 4). The reaction of $Mn^{II}(salen)$ with O_2 is a thermodynamically favorable process, which drives the electron transfer equilibrium (eq 2) in favor of $Mn^{II}(salen)$ and $Mn^{IV}(salen)(O)$. The remaining $Mn^{IV}(salen)(O)$ complex is dimerized to yield the same $[Mn^{IV}(salen)]_2(\mu\text{-}O)_2$ product (eq 3), but the origin of the bridging oxygen atoms is OH^-. According to Scheme 2, half of the di-μ-oxo ligands comes from O_2 and the other half comes from OH^-, although the experimental ^{18}O incorporation (Table 1) is somewhat deviated from this expectation.

The present $Mn^{III}(salen)(Cl)$ complex has a relatively rigid N_2O_2 plane around manganese, but yields the strained $[Mn^{IV}(salen)]_2(\mu\text{-}O)_2$ complex in which one of the phenolate oxygen atoms is forced to move to the axial position. In the case of the reaction with O_2 (eq 4, Scheme 2), the presence of the O−O bond in the reactant is a main factor for such a strained structure. Likewise, it is strongly expected that the O−O bond cleavage is also involved in the formation of strained $[Mn^{IV}(salen)]_2(\mu\text{-}O)_2$ from the reaction of $Mn^{III}(salen)(Cl)$ with OH^- (eq 3, Scheme 2). Indeed, the monomeric $Mn^{IV}(salen)(Cl)_2$ complex bearing the manganese(IV) center[59,60] was hydrolyzed with aqueous alkaline solution, but the $[Mn^{IV}(salen)]_2(\mu\text{-}O)_2$ complex was not formed. The formation of strained $[Mn^{IV}(salen)]_2(\mu\text{-}^{18}O)_2$ from the reaction of $Mn^{III}(salen)(Cl)$ with $^{18}OH^-$ is indicative of some reaction to

DOI: 10.1021/acs.inorgchem.5b01025
Inorg. Chem. 2015, 54, 8356−8366

Scheme 3. Reaction of Mn^{III}(salen) (Cl) with OH^- under Ar

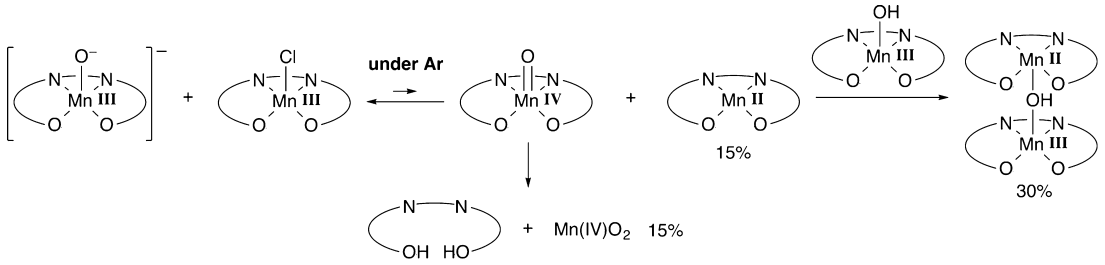

Scheme 4. A Proposed Mechanism of the Reaction of Mn^{III}(salen) (Cl) with OH^- in the Presence of Chloranil

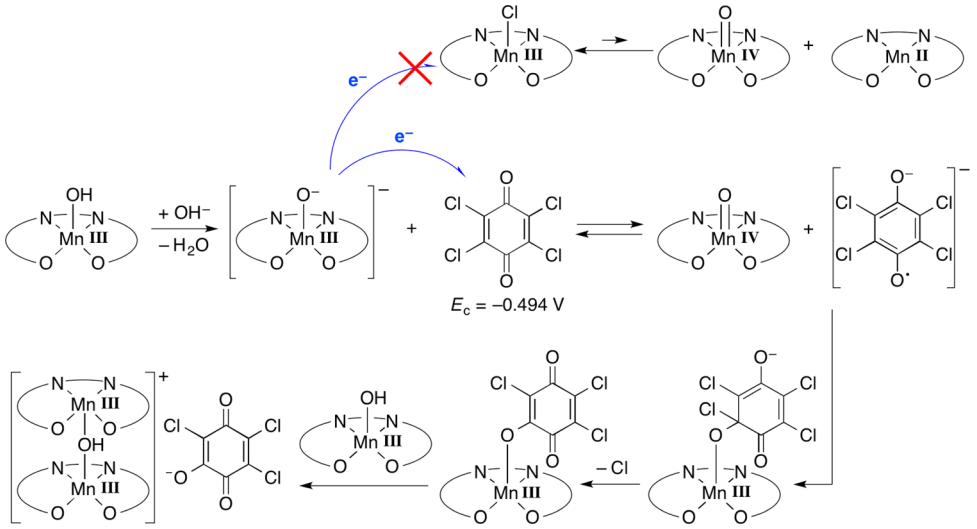

generate a peroxide species having a $^{18}O-^{18}O$ bond from two $^{18}OH^-$. In eq 3 (Scheme 2), the O−O bond formation is formally described as the dimerization of Mn^{IV}(salen)(O). The O−O bond formation was indeed observed for a Mn^{V}=O porphyrin dimer, which was ascribed to a coupling reaction between two high-valent Mn^{V}=O species or a nucleophilic attack of H_2O on Mn^{V}=O.[61] More recently, it was also reported that the O−O bond formation occurs as a consequence of a nucleophilic attack of OH^- on a monomeric Mn^{V}=O corrole.[62,63] The formation of a peroxide species from the reduction of O_2 as well as the oxidation of OH^- is exactly the reverse of a catalase-like reaction.

Further Insight into the Reaction Sequences. Control experiments were performed to gain further insight into the present reverse catalase reaction. One is the reaction of Mn^{III}(salen)(Cl) with OH^- in the absence of O_2. Under Ar atmosphere, the product is a μ-OH-bridged Mn^{II}/Mn^{III} dimer, [Mn^{II}(salen)][Mn^{III}(salen)](μ-OH), in low yield (30%), and the [Mn^{IV}(salen)]$_2$(μ-O)$_2$ product is not formed at all. Even under Ar atmosphere, the electron-transfer equilibrium between [Mn^{III}(salen)(O)]$^-$/Mn^{III}(salen)(Cl) and Mn^{IV}(salen)(O)/Mn^{II}(salen) (eq 2, Scheme 2) is established in exactly the same manner as under air. But the absence of O_2 precludes the conversion from Mn^{II}(salen) to [Mn^{IV}(salen)]$_2$(μ-O)$_2$ (eq 4, Scheme 2), which is the key reaction that drives the electron-transfer equilibrium in favor of Mn^{IV}(salen)(O) and Mn^{II}(salen). A limited amount of Mn^{IV}(salen)(O) generated under Ar is not enough to promote the conversion from Mn^{IV}(salen)(O) to [Mn^{IV}(salen)]$_2$(μ-O)$_2$ (eq 3, Scheme 2), resulting in no ^{18}O incorporation from $^{18}OH^-$ after the workup under air. Thus, the anaerobic conditions inhibit both routes leading to the formation of [Mn^{IV}(salen)]$_2$(μ-O)$_2$. The O_2 molecule plays an important role not only in generating [Mn^{IV}(salen)]$_2$(μ-O)$_2$ from the reaction with Mn^{II}(salen) but also in promoting the reaction of Mn^{IV}(salen)(O) to yield [Mn^{IV}(salen)]$_2$(μ-O)$_2$. This explains quite well one of the unique features of the present reverse catalase reaction, in which the two-electron oxidation of OH^- is coupled with the two-electron reduction of O_2.

The formation of [Mn^{II}(salen)][Mn^{III}(salen)](μ-OH) under Ar is ascribed to the ease of demetalation for Mn^{IV}(salen)(O) relative to Mn^{II}(salen) under the alkaline reaction conditions (Scheme 3). Under Ar atmosphere, the free salen ligand as a result of the demetalation is observed with ^1H NMR (Figure S13). The demetalation of Mn^{IV}(salen)(O) produces an equimolar amount of Mn^{II}(salen). The reaction of Mn^{II}(salen) with Mn^{III}(salen)(OH) yields [Mn^{II}(salen)][Mn^{III}(salen)](μ-OH).

The other control experiment to note is the addition of quinones, which altered the yield of [Mn^{IV}(salen)]$_2$(μ-O)$_2$ depending on the redox potential of quinones (Table 2). In the case of chloranil with highest oxidizing ability among three quinones tested, the [Mn^{IV}(salen)]$_2$(μ-O)$_2$ product was not obtained, and instead the [Mn^{III}(salen)]$_2$(μ-OH)(X) complex was detected as a major product. A primary role of chloranil is a quencher for the reducing [Mn^{III}(salen)(O)]$^-$ species and prevents the formation of a pair of Mn^{IV}(salen)(O) and Mn^{II}(salen) (Scheme 4). The addition of only 1 equiv of chloranil completely suppresses the formation of [Mn^{IV}(salen)]$_2$(μ-O)$_2$, which is consistent with the Mn-(salen)-based reductant for O_2 but is not compatible with the

DOI: 10.1021/acs.inorgchem.5b01025
Inorg. Chem. 2015, 54, 8356−8366

OH^- reductant, because a large excess of OH^- relative to chloranil is utilized.

The quenching of $[Mn^{III}(salen)(O)]^-$ blocks one of the routes to $[Mn^{IV}(salen)]_2(\mu\text{-}O)_2$ (the reaction of $Mn^{II}(salen)$ with O_2). But the addition of chloranil cannot prevent the formation of $Mn^{IV}(salen)(O)$, which is also a precursor to the $[Mn^{IV}(salen)]_2(\mu\text{-}O)_2$ product. Complete suppression of the formation of $[Mn^{IV}(salen)]_2(\mu\text{-}O)_2$ is indicative of a reaction of $Mn^{IV}(salen)(O)$ with one-electron reduced chloranil as shown in Scheme 4. The resulting $Mn^{III}(salen)$ complex reacts with $Mn^{III}(salen)(OH)$ to generate $[Mn^{III}(salen)]_2(\mu\text{-}OH)(X)$, which is unable to produce the reducing $[Mn^{III}(salen)(O)]^-$ species.

Complete quenching of the reaction by chloranil indicates that the oxidation potential of the $[Mn^{III}(salen)(O)]^-$ intermediate is more negative than the reduction potential of chloranil (E_o, −0.494 V vs Fc/Fc^+). In contrast, the oxidation potential of $[Mn^{III}(salen)(O)]^-$ is less negative than the reduction potential of *p*-benzoquinone (−1.042 V vs Fc/Fc^+), because the reaction is not altered at all upon the addition of *p*-benzoquinone. Partial quenching of the reaction by 2,5-dichloro-1,4-benzoquinone suggests that the reducing ability of $[Mn^{III}(salen)(O)]^-$ is close to the reduction potential of 2,5-dichloro-1,4-benzoquinone (−0.711 V vs Fc/Fc^+). In the presence of 2,5-dichloro-1,4-benzoquinone, the $[Mn^{III}(salen)(O)]^-$ intermediate reduces not only 2,5-dichloro-1,4-benzoquinone but also $Mn^{III}(salen)(Cl)$, which leads to the formation of $[Mn^{IV}(salen)]_2(\mu\text{-}O)_2$ in a lower yield.

CONCLUSION

The present study shows the feasibility of the reverse catalase reaction. In this reaction, the two electrons that are required for the O_2 reduction are provided from the formal oxidation of OH^- in aqueous alkaline solution. The present ^{18}O experiments shows that the O atoms in OH^- are incorporated into the $[Mn^{IV}(salen)]_2(\mu\text{-}O)_2$ complex most probably via the μ-peroxo dimanganese(III) complex, $[Mn^{III}(salen)]_2(\mu\text{-}O_2)$. The O_2 molecule is also incorporated into $[Mn^{IV}(salen)]_2(\mu\text{-}O)_2$ via the same $[Mn^{III}(salen)]_2(\mu\text{-}O_2)$ intermediate. The reverse catalase reaction has a great potential as the most efficient O_2 activation reaction, in which both O_2 and OH^- could be converted to oxidizing species. The present finding is quite an encouraging result for future challenges to explore aerobic oxygenation reactions operating under the new mechanism proposed here.

EXPERIMENTAL SECTION

Instrumentation. Resonance Raman spectra were measured with an inVia Reflex laser Raman microscope (RENISHAW). Raman shifts were calibrated with single-crystal silicon (520.3 cm^{-1}) for each measurement. Measurements were performed using the excitation wavelength of 532 nm, and the laser power of 0.5% (ca. 35 μW at the sample). Each spectrum was obtained with exposure time of 10 s and 10 accumulations. The rR spectra shown in this manuscript are the sum of five spectra, which were measured at different spots of each sample to minimize sample damage due to the laser irradiation. IR spectra were measured under vacuum with an IFS66v/S FT-IR spectrometer (Bruker). In the region from 400 to 800 cm^{-1}, IR spectra were obtained for KBr pellets at a resolution of 2 cm^{-1} as a sum of 32 scans. In the region from 100 to 700 cm^{-1}, IR spectra were obtained for CsI pellets at a resolution of 2 cm^{-1} as a sum of 128 scans. ESI-MS spectra were obtained with a LCT time-of-flight mass spectrometer equipped with an electrospray ionization interface (Micromass). Samples dissolved in CH_2Cl_2 were injected into the electrospray ionization interface. The cone voltage is 5 V. MALDI-MS spectra were measured with a Voyager DE-STR mass spectrometer (Applied Biosystems) using dithranol as a matrix substance. ^1H and ^2H NMR spectra were measured in a borosilicate glass tube (5 mm OD) on an LA-500 spectrometer (JEOL). ^1H and ^2H NMR chemical shifts in CD_2Cl_2 and CH_2Cl_2 were referenced to $CHDCl_2$ (5.32 ppm). ^1H NMR chemical shifts in $CDCl_3$ were referenced to $CHCl_3$ (7.24 ppm). Perpendicular- and parallel-mode EPR spectra were recorded for 50 μL of the frozen CH_2Cl_2 solution in a quartz cell (5 mm OD) on an EMX Plus continuous-wave X-band spectrometer (Bruker) with an ESR 910 helium-flow cryostat (Oxford Instruments) and a dual-mode cavity (Bruker). Simulations of EPR spectra were done by using the EasySpin program.[45] Cyclic voltammograms were measured with a Model 2325 electrochemical analyzer (BAS) using an Ag/Ag^+ reference electrode, a glassy-carbon working-electrode, and a platinum-wire counter electrode. Measurements were performed for the 1 mM solution in dehydrated CH_2Cl_2 containing 0.1 M Bu_4NOTf at a scan rate of 50 mV s^{-1} at 298 K under Ar atmosphere unless otherwise noted. The *E* values were referenced to the $E_{1/2}$ value of ferrocene, which was measured under identical conditions each time. Absorption spectra were recorded in anhydrous CH_2Cl_2 using a quartz cell (l = 0.1 cm) on an Agilent 8453 spectrometer (Agilent Technologies). Elemental analyses were conducted on a Micro Corder JM10 (J-Science Lab).

Materials. CD_2Cl_2 and $CDCl_3$ were purchased from ACROS. NaH dispersed in paraffin liquid was purchased from Nacalai. Benzyl alcohol, aluminum oxide (basic, Brockmann I, activated), and (*R,R*)-*N,N′*-bis(3,5-di-*tert*-butylsalicylidene)-1,2-cyclohexanediaminomanganese(III) chloride were purchased from Aldrich and were used as received. Other reagents were purchased from Kanto or Wako and were utilized as received. CD_2Cl_2, $CDCl_3$, and CH_2Br_2 were passed though aluminum oxide just before use. The preparation of $Mn^{III}(salen)(OTf)$ was previously reported.[59] $H_2{}^{18}O$ and $^{18}O_2$ (98%) were purchased from Cambridge Isotope Laboratories and were used as received. The preparations of selectively deuterated salen ligands (salen-d_2 and salen-d_4) were reported previously.[59,60]

Reaction of $Mn^{III}(salen)(Cl)$ with $Na^{18}OH$ under Air or Ar. 2.0 M $Na^{18}OH$ in $H_2{}^{18}O$ was prepared by carefully adding NaH dispersed in paraffin liquid (55%, 88 mg, 2.0 mmol) to $H_2{}^{18}O$ (1 mL). The resulting solution was washed with anhydrous toluene (3 mL × 3) to remove paraffin liquid. The $Mn^{III}(salen)(Cl)$ complex (100 mg, 0.157 mmol) dissolved in anhydrous toluene (5 mL) was then vigorously washed with 2.0 M $Na^{18}OH$ in $H_2{}^{18}O$ (1 mL). The toluene layer was dried over $MgSO_4$. After filtration, the solvent was removed by evaporation under reduced pressure. After the residue was dried in vacuo, the residue, dissolved in toluene (2 mL), was passed through a membrane filter (Millex-FG, pore size 0.45 mm, diameter 13 mm, Millipore). After the solvent was removed and the residue was dried in vacuo, anhydrous CH_3CN (5 mL) was added. The resulting suspension was heated to reflux for 10 min. The hot suspension was then filtered to afford a partially ^{18}O-labeled $[Mn^{IV}(salen)]_2(\mu\text{-}O)_2$ product (20 mg) after the product was dried in vacuo.

In the case of the reaction under Ar, the solution of $Mn^{III}(salen)(Cl)$ (100 mg, 0.157 mmol) in anhydrous toluene (5 mL) and 2.0 M $Na^{18}OH$ in $H_2{}^{18}O$ (1 mL) were separately degassed by three freeze−thaw cycles under Ar. The toluene solution of $Mn^{III}(salen)(Cl)$ was added via a gastight syringe to the 2.0 M $Na^{18}OH$ in $H_2{}^{18}O$ under Ar. The organic and aqueous layers were vigorously mixed. The organic layer was separated using a membrane filter (Universal Phase Separator, Biotage) under Ar. The organic layer was then placed under air for 4 h. After removing the solvent and drying the residue in vacuo, anhydrous CH_3CN (5 mL) was added. The resulting suspension was heated to reflux for 10 min. The hot suspension was then filtered to afford a nonlabeled $[Mn^{IV}(salen)]_2(\mu\text{-}O)_2$ product (11 mg) after the product was dried in vacuo.

Reaction of $Mn^{III}(salen)(Cl)$ with KOH or $Na^{18}OH$ under $^{18}O_2$. The toluene solution of $Mn^{III}(salen)(Cl)$ (200 mg, 0.315 mmol in 10 mL) and 2.0 M KOH aqueous solution (10 mL) were separately degassed by three freeze−thaw cycles under Ar. 2.0 M KOH aqueous solution was then placed under $^{18}O_2$ atmosphere for 1 h in a round-

DOI: 10.1021/acs.inorgchem.5b01025
Inorg. Chem. 2015, 54, 8356−8366

bottom flask that was connected to a $^{18}O_2$ bottle via a three-way cock and a vacuum tubing. The toluene solution of Mn^{III}(salen)(Cl) was added via a gastight syringe to the 2.0 M KOH aqueous solution under $^{18}O_2$. The organic and aqueous layers were vigorously mixed, and then the resulting biphasic mixture was placed under $^{18}O_2$ for 30 min. The organic layer was separated using a membrane filter (Universal Phase Separator, Biotage) under Ar. The solvent was removed in vacuo. The residue was dissolved in degassed CH_3CN under Ar. A partially ^{18}O-labeled $[Mn^{IV}(salen)]_2(\mu\text{-}O)_2$ product (18 mg) was obtained as a precipitate after the product was dried in vacuo.

The $[Mn^{IV}(salen)]_2(\mu\text{-}^{18}O)_2$ complex was obtained by the reaction of Mn^{III}(salen)(Cl) (100 mg, 0.157 mmol) in anhydrous toluene (5 mL) with 2.0 M $Na^{18}OH$ in $H_2{}^{18}O$ (1 mL) under $^{18}O_2$ atmosphere. 2.0 M $Na^{18}OH$ in $H_2{}^{18}O$ was prepared by carefully adding NaH dispersed in paraffin liquid (55%, 88 mg, 2.0 mmol) to $H_2{}^{18}O$ (1 mL). The resulting solution was washed with anhydrous toluene (3 mL × 3) to remove paraffin liquid.

Anaerobic Reaction of Mn^{III}(salen)(Cl) with KOH. The EPR sample was prepared as follows. The toluene solution of Mn^{III}(salen)(Cl) (254 mg, 0.40 mmol in 20 mL) and 2.0 M KOH aqueous solution (20 mL) were separately degassed by three freeze−thaw cycles under Ar. The toluene solution of Mn^{III}(salen)(Cl) was added via a gastight syringe to the 2.0 M KOH aqueous solution under Ar. The organic and aqueous layers were vigorously mixed. The organic layer was separated using a membrane filter (Universal Phase Separator, Biotage) under Ar. The resulting solution was then passed through a membrane filter (Millex-FG, pore size 0.45 mm, diameter 13 mm, Millipore) under Ar. An aliquot (100 μL) of the resulting solution was transferred to the EPR tube (5 mm OD), which was flame-sealed under reduced pressure.

The NMR sample was prepared as follows. The solution of Mn^{III}(salen)(Cl) (95 mg, 0.15 mmol) in toluene-d_8 (3 mL) and 2.0 M KOH aqueous solution (20 mL) were separately degassed by three freeze−thaw cycles under Ar. The toluene-d_8 solution of Mn^{III}(salen)(Cl) was added via a gastight syringe to the 2.0 M KOH aqueous solution under Ar. The organic and aqueous layers were vigorously mixed. The organic layer was separated using a membrane filter (Universal Phase Separator, Biotage) under Ar. The resulting solution was then passed through a membrane filter (Millex-FG, pore size 0.45 mm, diameter 13 mm, Millipore) under Ar. An aliquot (600 μL) of the resulting solution was transferred to the low vacuum/pressure NMR tube (Wilmad) for ^{1}H NMR measurements.

Quantitative Analyses of $[Mn^{IV}(salen)]_2(\mu\text{-}O)_2$. The reactions of Mn^{III}(salen)(Cl) with 2.0 M KOH aqueous solution in the presence of oxidants or reductants were done as follows. The solution of Mn^{III}(salen)(Cl) (50 mg, 79 μmol) and 1 equiv of an additive in toluene (5 mL) was vigorously washed with 2.0 M KOH aqueous solution (5 mL). The organic layer was separated using a membrane filter (Universal Phase Separator, Biotage). The solvent was removed by evaporation under reduced pressure. After the residue was dried in vacuo, the yield of $[Mn^{IV}(salen)]_2(\mu\text{-}O)_2$ was determined with ^{1}H NMR in $CDCl_3$ using CH_2Br_2 as an internal standard. Reported yields are averaged values from three independent experiments.

Preparation of $[Mn^{III}(salen)]_2(\mu\text{-}OH)(OTf)$. The aluminum oxide (basic, Brockmann I, activated, 9.00 g) and H_2O (1.8 mL) in CH_2Cl_2 (60 mL) was well-sonicated. To the resulting suspension was added the Mn^{III}(salen)(OTf) complex (875 mg, 1.16 mmol). The mixture was stirred at room temperature for 6 h. After filtration, the solvent was removed by evaporation under reduced pressure. The residue dissolved in CH_2Cl_2 (ca. 5 mL) was passed through a membrane filter (Millex-FG, pore size 0.45 mm, diameter 13 mm, Millipore). The addition of pentane (ca. 50 mL) gave the $[Mn^{III}(salen)]_2(\mu\text{-}OH)(OTf)$ complex as a precipitate (676 mg, 0.489 mmol). Anal. Calcd for $C_{73}H_{105}F_3Mn_2N_4O_8S{\cdot}H_2O$: C, 63.37; H, 7.80; N, 4.05. Found: C, 63.37; H, 7.75; N, 4.02%.

The ^{2}H-labeled complexes for ^{2}H NMR were prepared from Mn^{III}(salen-d_4)(OTf) and Mn^{III}(salen-d_2)(OTf) in exactly the same manner. The ^{2}H-labeled complexes were used for ^{2}H NMR measurements without purification.

The μ-^{18}OH and μ-^{2}HO complexes were prepared using $H_2{}^{18}O$ and ^2H_2O instead of H_2O. The products were used without purification for ^{2}H NMR, rR, and IR measurements.

■ ASSOCIATED CONTENT

Ⓢ Supporting Information

The Supporting Information is available free of charge on the ACS Publications website at DOI: 10.1021/acs.inorgchem.5b01025.

^{1}H NMR, mass, Raman, absorption, X-band EPR, and IR spectra, illustrated atom numbering scheme for selectively deuterated salen, ^{2}H NMR Curie plots, cyclic voltammograms. (PDF)

■ AUTHOR INFORMATION

Corresponding Author

*E-mail: kurahasi@ims.ac.jp.

Notes

The authors declare no competing financial interest.

■ ACKNOWLEDGMENTS

This work was supported by JSPS KAKENHI Grant Nos. 23550086 and 15K05462. The financial support from the Naito Foundation is gratefully acknowledged. I thank Prof. H. Fujii (Nara Women's Univ.) for encouragement with this work.

■ REFERENCES

(1) Lippard, S. J.; Berg, J. M. *Principles of Bioinorganic Chemistry;* University Science Books: New York, 1994.

(2) Nguyen, A. I.; Hadt, R. G.; Solomon, E. I.; Tilley, T. D. *Chem. Sci.* **2014**, *5*, 2874−2878.

(3) Dai, F.; Yap, G. P. A.; Theopold, K. H. *J. Am. Chem. Soc.* **2013**, *135*, 16774−16776.

(4) Coggins, M. K.; Sun, X.; Kwak, Y.; Solomon, E. I.; Rybak-Akimova, E.; Kovacs, J. A. *J. Am. Chem. Soc.* **2013**, *135*, 5631−5640.

(5) Cho, Y. I.; Joseph, D. M.; Rose, M. J. *Inorg. Chem.* **2013**, *52*, 13298−13300.

(6) Hong, S.; Lee, Y.-M.; Shin, W.; Fukuzumi, S.; Nam, W. *J. Am. Chem. Soc.* **2009**, *131*, 13910−13911.

(7) Nishida, Y.; Lee, Y.-M.; Nam, W.; Fukuzumi, S. *J. Am. Chem. Soc.* **2014**, *136*, 8042−8049.

(8) Li, F.; Van Heuvelen, K. M.; Meier, K. K.; Münck, E.; Que, L., Jr. *J. Am. Chem. Soc.* **2013**, *135*, 10198−10201.

(9) Lee, Y.-M.; Hong, S.; Morimoto, Y.; Shin, W.; Fukuzumi, S.; Nam, W. *J. Am. Chem. Soc.* **2010**, *132*, 10668−10670.

(10) Thibon, A.; England, J.; Martinho, M.; Young, V. G., Jr.; Frisch, J. R.; Guillot, R.; Girerd, J.-J.; Münck, E.; Que, L., Jr.; Banse, F. *Angew. Chem., Int. Ed.* **2008**, *47*, 7064−7067.

(11) Liu, S.; Mase, K.; Bougher, C.; Hicks, S. D.; Abu-Omar, M. M.; Fukuzumi, S. *Inorg. Chem.* **2014**, *53*, 7780−7788.

(12) Liu, J.-G.; Shimizu, Y.; Ohta, T.; Naruta, Y. *J. Am. Chem. Soc.* **2010**, *132*, 3672−3673.

(13) Ségaud, N.; Anxolabéhère-Mallart, E.; Sénéchal-David, K.; Acosta-Rueda, L.; Robert, M.; Banse, F. *Chem. Sci.* **2015**, *6*, 639−647.

(14) Ching, H. Y. V.; Anxolabéhère-Mallart, E.; Colmer, H. E.; Costentin, C.; Dorlet, P.; Jackson, T. A.; Policar, C.; Robert, M. *Chem. Sci.* **2014**, *5*, 2304.

(15) Asahi, M.; Yamazaki, S.; Itoh, S.; Ioroi, T. *Dalton Trans.* **2014**, *43*, 10705−10709.

(16) Kim, S. O.; Sastri, C. V.; Seo, M. S.; Kim, J.; Nam, W. *J. Am. Chem. Soc.* **2005**, *127*, 4178−4179.

(17) MacDonnell, F. M.; Fackler, N. L. P.; Stern, C.; O'Halloran, T. V. *J. Am. Chem. Soc.* **1994**, *116*, 7431−7432.

(18) Mahammed, A.; Gray, H. B.; Meier-Callahan, A. E.; Gross, Z. *J. Am. Chem. Soc.* **2003**, *125*, 1162−1163.

DOI: 10.1021/acs.inorgchem.5b01025
Inorg. Chem. 2015, 54, 8356−8366

(19) Heier, P.; Boscher, N. D.; Choquet, P.; Heinze, K. *Inorg. Chem.* **2014**, *53*, 11086−11095.
(20) O'Reilly, M. E.; Del Castillo, T. J.; Falkowski, J. M.; Ramachandran, V.; Pati, M.; Correia, M. C.; Abboud, K. A.; Dalal, N. S.; Richardson, D. E.; Veige, A. S. *J. Am. Chem. Soc.* **2011**, *133*, 13661−13673.
(21) Ghosh, A.; Tiago de Oliveira, F.; Yano, T.; Nishioka, T.; Beach, E. S.; Kinoshita, I.; Münck, E.; Ryabov, A. D.; Horwitz, C. P.; Collins, T. J. *J. Am. Chem. Soc.* **2005**, *127*, 2505−2513.
(22) Lippert, C. A.; Arnstein, S. A.; Sherrill, C. D.; Soper, J. D. *J. Am. Chem. Soc.* **2010**, *132*, 3879−3892.
(23) Jung, J.; Ohkubo, K.; Prokop-Prigge, K. A.; Neu, H. M.; Goldberg, D. P.; Fukuzumi, S. *Inorg. Chem.* **2013**, *52*, 13594−13604.
(24) Prokop, K. A.; Goldberg, D. P. *J. Am. Chem. Soc.* **2012**, *134*, 8014−8017.
(25) Vanover, E.; Huang, Y.; Xu, L.; Newcomb, M.; Zhang, R. *Org. Lett.* **2010**, *12*, 2246−2249.
(26) Harischandra, D. N.; Lowery, G.; Zhang, R.; Newcomb, M. *Org. Lett.* **2009**, *11*, 2089−2092.
(27) Rosenthal, J.; Luckett, T. D.; Hodgkiss, J. M.; Nocera, D. G. *J. Am. Chem. Soc.* **2006**, *128*, 6546−6547.
(28) Pistorio, B. J.; Chang, C. J.; Nocera, D. G. *J. Am. Chem. Soc.* **2002**, *124*, 7884−7885.
(29) Maiti, B. K.; Maia, L. B.; Pal, K.; Pakhira, B.; Avilés, T.; Moura, I.; Pauleta, S. R.; Nuñez, J. L.; Rizzi, A. C.; Brondino, C. D.; Sarkar, S.; Moura, J. J. G. *Inorg. Chem.* **2014**, *53*, 12799−12808.
(30) Choi, K. S.; Lai, T. H.; Lee, S. Y.; Chan, K. S. *Organometallics* **2011**, *30*, 2633−2635.
(31) Arasasingham, R. D.; Bruice, T. C. *Inorg. Chem.* **1990**, *29*, 1422−1427.
(32) Shin, K.; Kramer, S. K.; Goff, H. M. *Inorg. Chem.* **1987**, *26*, 4103−4106.
(33) Srivatsa, G. S.; Sawyer, D. T. *Inorg. Chem.* **1985**, *24*, 1732−1734.
(34) Fukuzumi, S.; Nakanishi, I.; Maruta, J.; Yorisue, T.; Suenobu, T.; Itoh, S.; Arakawa, R.; Kadish, K. M. *J. Am. Chem. Soc.* **1998**, *120*, 6673−6680.
(35) Fukuzumi, S.; Yorisue, T. *J. Am. Chem. Soc.* **1991**, *113*, 7764−7765.
(36) McGarrigle, E. M.; Gilheany, D. G. *Chem. Rev.* **2005**, *105*, 1563−1602.
(37) Larson, E. J.; Pecoraro, V. L. *J. Am. Chem. Soc.* **1991**, *113*, 3810−3818.
(38) Kurahashi, T.; Hada, M.; Fujii, H. *Inorg. Chem.* **2014**, *53*, 1070−1079.
(39) Holland, P. L.; Cramer, C. J.; Wilkinson, E. C.; Mahapatra, S.; Rodgers, K. R.; Itoh, S.; Taki, M.; Fukuzumi, S.; Que, L., Jr.; Tolman, W. B. *J. Am. Chem. Soc.* **2000**, *122*, 792−802.
(40) Wilkinson, E. C.; Dong, Y.; Zang, Y.; Fujii, H.; Fraczkiewicz, R.; Fraczkiewicz, G.; Czernuszewicz, R. S.; Que, L., Jr. *J. Am. Chem. Soc.* **1998**, *120*, 955−962.
(41) Dave, B. C.; Czernuszewicz, R. S. *Inorg. Chim. Acta* **1994**, *227*, 33−41.
(42) Hasegawa, K.; Ono, T. *Bull. Chem. Soc. Jpn.* **2006**, *79*, 1025−1031.
(43) Kurahashi, T.; Fujii, H. *Bull. Chem. Soc. Jpn.* **2012**, *85*, 940−947.
(44) Dismukes, G. C.; Sheats, J. E.; Smegal, J. A. *J. Am. Chem. Soc.* **1987**, *109*, 7202−7203.
(45) Stoll, S.; Schweiger, A. *J. Magn. Reson.* **2006**, *178*, 42−55.
(46) Smith, S. J.; Riley, M. J.; Noble, C. J.; Hanson, G. R.; Stranger, R.; Jayaratne, V.; Cavigliasso, G.; Schenk, G.; Gahan, L. R. *Inorg. Chem.* **2009**, *48*, 10036−10048.
(47) Huang, P.; Shaikh, N.; Anderlund, M. F.; Styring, S.; Hammarström, L. *J. Inorg. Biochem.* **2006**, *100*, 1139−1146.
(48) Diril, H.; Chang, H.-R.; Nilges, M. J.; Zhang, X.; Potenza, J. A.; Schugar, H. J.; Isied, S. S.; Hendrickson, D. N. *J. Am. Chem. Soc.* **1989**, *111*, 5102−5114.
(49) Schäfer, K.-O.; Bittl, R.; Lendzian, F.; Barynin, V.; Weyhermüller, T.; Wieghardt, K.; Lubitz, W. *J. Phys. Chem. B* **2003**, *107*, 1242−1250.
(50) Limburg, J.; Vrettos, J. S.; Liable-Sands, L. M.; Rheingold, A. L.; Crabtree, R. H.; Brudvig, G. W. *Science* **1999**, *283*, 1524−1527.
(51) Gallo, E.; Solari, E.; Re, N.; Floriani, C.; Chiesi-Villa, A.; Rizzoli, C. *J. Am. Chem. Soc.* **1997**, *119*, 5144−5154.
(52) Horwitz, C. P.; Winslow, P. J.; Warden, J. T.; Lisek, C. A. *Inorg. Chem.* **1993**, *32*, 82−88.
(53) Horwitz, C. P.; Ciringh, Y.; Liu, C.; Park, S. *Inorg. Chem.* **1993**, *32*, 5951−5956.
(54) Dailey, G. C.; Horwitz, C. P.; Lisek, C. A. *Inorg. Chem.* **1992**, *31*, 5325−5330.
(55) Sawyer, D. T.; Roberts, J. L., Jr. *Acc. Chem. Res.* **1988**, *21*, 469−476.
(56) Taguchi, T.; Gupta, R.; Lassalle-Kaiser, B.; Boyce, D. W.; Yachandra, V. K.; Tolman, W. B.; Yano, J.; Hendrich, M. P.; Borovik, A. S. *J. Am. Chem. Soc.* **2012**, *134*, 1996−1999.
(57) Parsell, T. H.; Yang, M.-Y.; Borovik, A. S. *J. Am. Chem. Soc.* **2009**, *131*, 2762−2763.
(58) Parsell, T. H.; Behan, R. K.; Green, M. T.; Hendrich, M. P.; Borovik, A. S. *J. Am. Chem. Soc.* **2006**, *128*, 8728−8729.
(59) Kurahashi, T.; Fujii, H. *J. Am. Chem. Soc.* **2011**, *133*, 8307−8316.
(60) Kurahashi, T.; Hada, M.; Fujii, H. *J. Am. Chem. Soc.* **2009**, *131*, 12394−12405.
(61) Shimazaki, Y.; Nagano, T.; Takesue, H.; Ye, B. H.; Tani, F.; Naruta, Y. *Angew. Chem., Int. Ed.* **2004**, *43*, 98−100.
(62) Kim, S. H.; Park, H.; Seo, M. S.; Kubo, M.; Ogura, T.; Klajn, J.; Gryko, D. T.; Valentine, J. S.; Nam, W. *J. Am. Chem. Soc.* **2010**, *132*, 14030−14032.
(63) Gao, Y.; Åkermark, T.; Liu, J.; Sun, L.; Åkermark, B. *J. Am. Chem. Soc.* **2009**, *131*, 8726−8727.

DOI: 10.1021/acs.inorgchem.5b01025
Inorg. Chem. 2015, 54, 8356−8366